Humidity Effects According to the Type of Carbon Nanotubes

YONGWOO LEE[ID]**, JINSU YOON, YEAMIN KIM, DONG MYONG KIM**[ID]**, (Member, IEEE), DAE HWAN KIM**[ID]**, (Senior Member, IEEE), AND SUNG-JIN CHOI**[ID]

School of Electrical Engineering, Kookmin University, Seoul 02707, South Korea

Corresponding author: Sung-Jin Choi (sjchoiee@kookmin.ac.kr)

ABSTRACT As a new type of one-dimensional nanomaterial, carbon nanotubes (CNTs) have been used as a chemical sensing material due to their excellent electrical, mechanical and chemical properties. Several recent studies have attempted to obtain an electrochemical sensor based on CNTs, and CNT-based humidity sensors have potential applications in industrial, agricultural and medical fields and in smart wearable electronic devices. Although various CNT-based humidity sensors have been reported, in this work, we investigated the humidity effects in depth and the underlying mechanisms according to CNT type, i.e., semiconducting (s-CNT) and metallic (m-CNT) CNTs, which is determined by the chiral vector during CNT growth. For this purpose, we fabricated CNT-based humidity sensors with highly purified, solution-processed 99% single-walled s-CNT and m-CNT network films bridged by palladium (Pd) electrodes. The fabricated sensors exhibited completely different humidity responses, as denoted by the film resistance as a function of the relative humidity (RH), according to the CNT type. In the s-CNT-based sensor, the resistance tended to decrease as the RH increased, while the m-CNT-based sensor showed the opposite tendency. Based on these results, a humidity sensing mechanism according to the CNT type was proposed in this work. We believe that our findings can serve as design guidelines for CNT-based humidity sensors.

INDEX TERMS Humidity sensor, semiconducting carbon nanotube, metallic carbon nanotube, network, Schottky barrier, charge transfer.

I. INTRODUCTION

The ability to monitor humidity in ambient air has become increasingly important recently and is essential in the fields of modern industrial and agricultural production, system control, quality storage, and medical care [1]–[4]. An ideal humidity sensor should have high sensitivity, fast responsivity, wide operating ranges, and excellent stability and reproducibility. To achieve these sensing performance requirements, sensors based on various nanomaterials have been proposed for use as high-performance humidity sensors [5]–[9]. Among them, carbon nanotube (CNT)-based humidity sensors have been an area of focus due to their attractive material properties, including high carrier mobility, excellent mechanical flexibility and stiffness, compatibility with solution-based processing, and large surface-to-volume

ratio [10]–[15]. In particular, CNTs have been demonstrated as many potential applications, including nanocomposites, membranes, electrodes, and sensors [16]–[21]. In addition, due to the structural advantages of one-dimensional CNTs over other nanomaterials, research on CNT-based humidity sensors has been actively performed [22]–[25]. However, most studies have been carried out in a percolation network film with a mixed state of semiconducting CNTs (s-CNTs) and metallic CNTs (m-CNTs); hence, to improve the sensing ability, it is necessary to study the detailed mechanism of the humidity response of each type of CNT. Recently, a two-terminal sensor based on two types of solution-processed CNTs (i.e., s- and m-CNTs) have been reported for changes in electrical current to saturated water vapor [26], but detail characterization by humidity responses and their sensing mechanism have not been investigated fully.

In this article, we fabricated two different resistive-type humidity sensors based on highly purified, preseparated

The associate editor coordinating the review of this manuscript and approving it for publication was Wuliang Yin[ID].

single-walled s-CNTs and m-CNTs. The CNTs were percolated, resulting in the formation of CNT networks, and they were bridged by palladium (Pd) electrodes. The changes in the electrical resistance of the sensors were measured at various relative humidity (RH) levels to compare the two sensors. Notably, the humidity responses of the two sensors to different RH levels exhibited exactly opposite trends. In the sensor based on s-CNTs, Schottky barrier modulation, which was the result of modifying the work function of the Pd electrodes upon exposure to moisture, was the major element in humidity sensing [27]. However, in the sensor based on m-CNTs, the dominant humidity effect was the electron charge transfer from the water (H_2O) molecules to the CNT channel due to the adsorption of H_2O molecules on the CNT surface [23]. In addition, s-CNT/m-CNT-based humidity sensors with copper (Cu) electrodes, which do not react with H_2O molecules, were also fabricated to verify each sensing mechanism. We expect that the observations in this work may significantly influence the design and operation of CNT-based humidity sensors for practical applications.
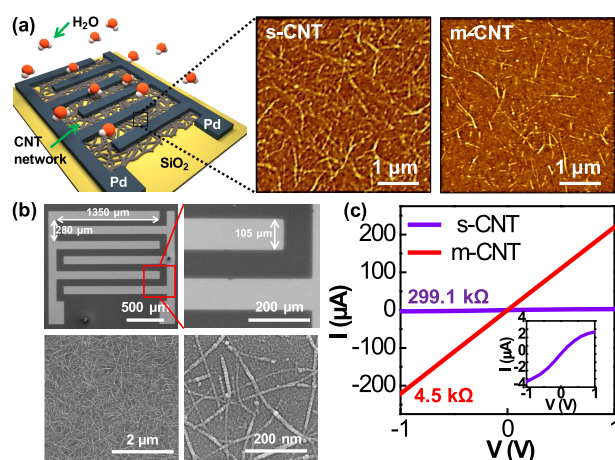

FIGURE 1. (a) Schematic of the fabricated humidity sensor structure. AFM images of a CNT network for a humidity sensing material: 99% s-CNT solution (left) and 99% m-CNT solution (right). (b) SEM images of the fabricated humidity sensor and the CNT networks. (c) Initial I-V curves of the fabricated humidity sensors with two different channel materials; the inset shows the magnified I-V curves of the s-CNT-based sensor. The resistance of the s-CNT-based sensor is much higher than that of the m-CNT-based sensor.

II. RESULTS AND DISCUSSION

Figure 1a shows a schematic of the CNT-based humidity sensors using s-CNTs and m-CNTs as sensing materials to compare the sensing responses in this study. To provide the necessary electrical contacts to measure the change in resistance depending on the RH levels, an interdigitated electrode structure was introduced in the CNT-based humidity sensor. The sensor was fabricated on 1.5 cm × 1.5 cm pieces of <100> oriented p-type silicon/silicon dioxide (Si/SiO_2) wafer substrates with resistivity less than 0.005 $\Omega \cdot$ cm and thickness of 525 μm (purchased from QL Electronics Co.). First, after cleaning the substrate, we performed oxygen plasma treatment to make the surface hydrophilic.

The SiO_2 surface was then functionalized by a poly-L-lysine solution (0.1% w/v in water; Sigma Aldrich) to form an amine-terminated layer and adhere the CNTs [28], [29]. Following a rinsing process with deionized (DI) water, the substrate was immersed in highly purified, preseparated single-walled 99% s-CNT and 99% m-CNT solutions (purchased from Nano Integris, Inc.) for 20 min to form randomly percolated CNT networks. Note that the preparation processes of the two types of CNT solutions are as follows: First, single-walled CNTs were produced by carbon monoxide (CO) disproportionation using a cobalt/molybdenum (Co/Mo) catalysts [30]. Then, the formed single-walled CNTs are separated into high-purity s-CNTs and m-CNTs through an additional density gradient ultracentrifugation method [31]. Then, the substrate was rinsed with isopropyl alcohol (IPA) and DI water for 1 min and 30 sec, respectively, and dried with flowing nitrogen. Atomic force microscopy (AFM) images of the two CNT networks consisting of s-CNTs and m-CNTs are shown in Figure 1a. The AFM images show that both networks are well formed by s-CNTs and m-CNTs on the SiO_2 surface. Finally, two interdigitated electrodes are formed by depositing a 40-nm-thick Pd layer with 99.99% purity (EPD0SW0005, TASCO Ltd.) via an e-beam evaporator under a pressure of 4×10^{-6} Torr at room temperature. Scanning electron microscopy (SEM) images of the CNT-based humidity sensor and a deposited CNT network are presented in Figure 1b. We used a finger width of 8 mm and an interelectrode distance of 100 μm in the sensors to measure the sensing responses. To compare the initial electrical characteristics of the sensors, we measured the current-voltage (I-V) curves of the two humidity sensors at room temperature, as shown in Figure 1c. From the initial resistance values obtained from the I-V curves, the s-CNT-based sensor has a significantly higher resistance than the m-CNT-based sensor. Regardless of the type of CNT, the differential resistance is constant over the operating voltage range; the sensitivity is identical regardless of the operation bias. That is, a low operating voltage does not hinder the sensitivity, thus allowing low-power operation.

Figure 2a shows the experimental setup used for humidity sensing measurements. The sensing responses of the CNT-based humidity sensors in a closed vacuum chamber were tested under different humidity conditions at room temperature. A thin connection tube placed in the chamber delivers the moisture-containing gas, and the RH level in the chamber was monitored in real time by a hygrometer (TH-05, Daekwang Instrument Inc.) at room temperature. We used mass flow controllers (MFCs) to control the humidity. Two MFCs were connected to the air gas: the air gas from MFC-1 flows directly to the sensor, and the air gas from MFC-2 flows into the sensor after passing through a saturated K_2SO_4 solution. The K_2SO_4 exists as K^+ and SO_4^{2-} ions in H_2O, which prevent H_2O molecules from escaping into the air. Upon passing through the K_2SO_4 solution, nitrogen (N_2) and oxygen (O_2) with high electronegativity contained in the air gas desorb K^+ and SO_4^{2-} ions surrounded by the H_2O molecules;
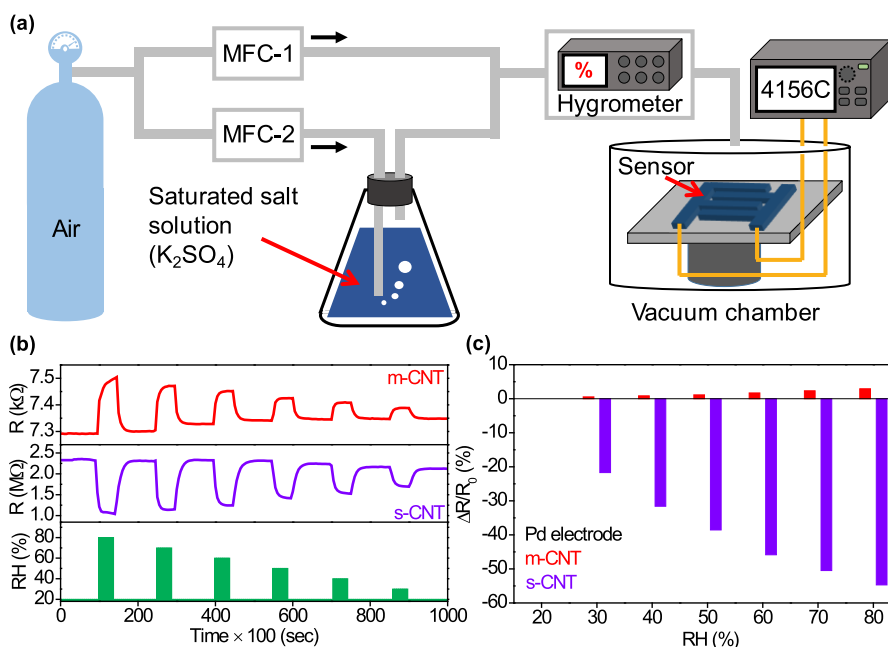
FIGURE 2. (a) Schematic illustrating the RH control setup for humidity sensing measurements. (b) Response curve of the m-CNT- and s-CNT-based humidity sensors under different RH levels (20%–80%). (c) Relative resistance change ($\Delta R/R_0$) of m-CNT- and s-CNT-based sensors according to RH level.

in this process, the H_2O molecules evaporate on the surface of the saturated K_2SO_4 solution, and the air gas changes from dry air to wet air [32], [33]. As a result, the required RH values can be acquired accurately by calibrating the two MFCs. Figure 2b illustrate the transient measurements of the s-CNT/m-CNT-based humidity sensors as a function of the RH level. In the measurements, we read out the 2-terminal resistance of the sensors in real time under a constant voltage of 0.5 V applied to our sensors using a parameter analyzer (Agilent 4156C). To observe the resistance changes with various humidity levels, we set the initial baseline RH value to 20% and measured the resistance changes while varying the RH level from 80% to 30%. The period of exposure to humidity was 40 sec, and the period of exposure to dried air was 100 sec. The fabricated sensors have a slight current drift that did not significantly affect sensor performance; hence, the sensing signal can be stably detected for adjustable RH levels ranging from 20% to 80%. During the measurements, we observed opposite trends for the two types of humidity sensors, as shown in Figure 2b. The resistance of the m-CNT-based sensor increases with increasing humidity, but the s-CNT-based sensor shows the opposite behavior. To better describe the resistance changes in response to humidity, we also plotted the relative change in resistance ($\Delta R/R_0$) under various humidity levels, where ΔR is the value of $R - R_0$, R is the instantaneous resistance when exposed to moisture, and R_0 is the initial resistance under dry conditions before exposure (RH = 20%). In Figure 2c, the two sensors clearly exhibited opposite responses under increasing

RH levels: a positive slope ($\delta(\Delta R/R_0)/\delta RH > 0$) for the m-CNT-based network and a negative slope ($\delta(\Delta R/R_0)/\delta RH < 0$) for the s-CNT-based network. The results for the m-CNT-based sensor can be explained by the change in the carrier density with a Fermi level (E_F) shift. Before exposure to moisture, the carrier density of the m-CNTs was increased under ambient air because the E_F of the m-CNT was shifted toward the van Hove singularity (vHs) with a high density of states (DOS) at the valence band due to the adsorption of O_2, which is a hole dopant [34], [35]. Therefore, when the m-CNTs predoped by O_2 absorption were exposed to moisture, which is an electron dopant, the hole-doping effect of the m-CNTs was compensated. Thus, as the RH level increases, the reduced carrier density due to the E_F being away from the vHs of the valence band resulted in the high resistance of the m-CNTs. Similar to the m-CNTs, the s-CNTs were also predoped by O_2 in ambient air. It has also been reported that H_2O can be adsorbed to CNT by oxygen defects such as carbonyl ($-CO$) groups formed on the CNT surface, and the charge (electron) is transferred from the adsorbed H_2O to the CNT [36]. Therefore, we expected that the s-CNTs would detect H_2O with the same mechanism as the m-CNTs. However, we observed that the resistance of the s-CNT-based sensor had the opposite tendency, as shown in Figure 2c. It can be inferred that this tendency of the s-CNT-based sensor is due to the existence of another mechanism. Unlike the m-CNT-based sensor, the s-CNT-based sensor had a Schottky barrier between the electrode and CNT; thus, the change in the metal (i.e., Pd) work function was also an important factor

in the s-CNT-based sensor response. Since Pd can absorb up to 900 times its own volume [37], [38], it is known that under hydrogen (H_2) conditions in ambient air, some portion of the Pd was changed to palladium hydride (PdH_X), which possesses a lower work function than that of the initial Pd electrode [39]. It is also reported that H_2O molecules are separated and adsorbed on Pd surface into OH groups, and that adsorbed OH groups are combined with the H in the PdH_X, helping the PdH_X convert back to Pd [27]. Therefore, we expected that preformed PdH_X in ambient air would be transformed back to Pd during the H_2O sensing experiment. The higher work function associated with the recovered Pd was beneficial to the transfer of holes from Pd to s-CNT due to the decrease in the Schottky barrier of the holes, resulting in a decrease in the overall resistance of the sensor. These interpretations and experimental results imply that the Schottky barrier change due to the work function change of the Pd electrode has a more dominant influence on the resistance change of the s-CNT-based sensor than does the carrier density change of the CNTs due to the doping effect. We also confirmed that the $\Delta R/R_0$ (54.7% at RH = 80%) of the s-CNT-based sensor was approximately 19 times larger than the $\Delta R/R_0$ (2.9% at RH = 80%) of the m-CNT-based sensor. This difference in $\Delta R/R_0$ might arise from the different current dependence of each element (carrier density and Schottky barrier), as described in the following equations:

$$I \propto qNv \tag{1}$$
$$I \propto e^{-q\phi_B/k_BT} \tag{2}$$

where q is the electron charge, N is the carrier density, v is the carrier velocity, ϕ_B is the Schottky barrier, k_B is the Boltzmann constant, and T is the temperature. As shown in equations 1 and 2, the change in current has a linear dependence on carrier density but has an exponential dependence on the Schottky barrier. Therefore, the observation showing that the current change of the s-CNT-based sensor is larger than that of the m-CNT-based sensor is valid because the s-CNT-based sensor detects H_2O by the change in the Schottky barrier.

To verify the mechanism of each sensor described above, we fabricated control sensors composed of copper (Cu) electrodes that do not react with H_2O. For the m-CNT-based sensor with Cu electrodes, the resistance increased with increasing RH, and the $\Delta R/R_0$ at RH = 80% was 3.2% (Figure 3). These results were very similar to those for the m-CNT-based sensor with Pd electrodes mentioned above. Therefore, we could confirm that the m-CNT-based sensor depends on only the change in carrier density of the CNTs according to the adsorption of H_2O regardless of the type of electrode. However, the s-CNT-based sensor with Cu electrodes had an opposite tendency to the s-CNT-based sensor with Pd electrodes, and this tendency was actually the same as that demonstrated by the m-CNT-based sensor with Pd electrodes, as shown in Figure 3. This result occurs because, unlike the work function of Pd, the work function of the
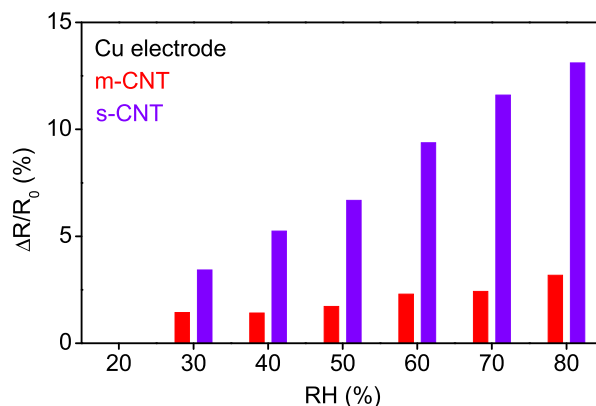

FIGURE 3. Relative resistance change ($\Delta R/R_0$) of m-CNT- and s-CNT-based sensors with Cu electrode according to RH levels.

Cu electrodes was not changed by the absorption of H_2O. Thus, these findings imply that for the sensor with Cu electrodes, the carrier density change of the s-CNTs by electron transfer is a more dominant mechanism than the change in the Schottky barrier. As a result, the measured $\Delta R/R_0$ (13.1% at RH = 80%) of the s-CNT-based sensor with the Cu electrodes is approximately 4 times smaller than $\Delta R/R_0$ of the s-CNT-based sensor with Pd electrodes.

Furthermore, we also observed that the $\Delta R/R_0$ values of the s-CNT-based sensor and the m-CNT-based sensor with Cu electrodes were different, although they detected H_2O through the same mechanism. This difference in $\Delta R/R_0$ was caused by the difference in the DOS distributions between the s-CNTs and m-CNTs. Since the carrier density in the CNTs is determined by the DOS in the vicinity of E_F, the relative rate of change in the DOS caused by the shift in E_F by H_2O practically produces a current change in the sensors. Unlike the s-CNTs, the m-CNTs do not have an energy band gap and have a constant DOS between the vHs of the conduction and valence bands [40]–[42]. Therefore, the relative rate of change in the DOS due to the shift in E_F by H_2O is larger for the s-CNTs than for the m-CNTs, resulting in the higher $\Delta R/R_0$ in the s-CNT-based sensors, even those with the Cu electrodes.

To investigate the repeatability of the fabricated sensor, we also performed cycling and hysteresis measurements on both the m-CNT and s-CNT-based sensors with the Pd electrodes (Figure 4). Figures 4a and 4b show resistance changes of the m-CNT- and s-CNT-based sensors as a function of time when the sensors were exposed to five cycles of a sequence of wet air (sensing for 40 sec) and dry air (recovery for 100 sec) according to several RH levels (30%, 40%, 50%, and 60%). It was found that the sensors did not have much sensing performance decay during the sensing cycles, which suggests that the sensing characteristics were repeatable. Moreover, the hysteresis characteristics of our sensors are also shown in Figures 4c and 4d. The open bars in Figures 4c and 4d represent the measurement conducted during hydration (sequentially increasing the RH level from 20% to 80%),
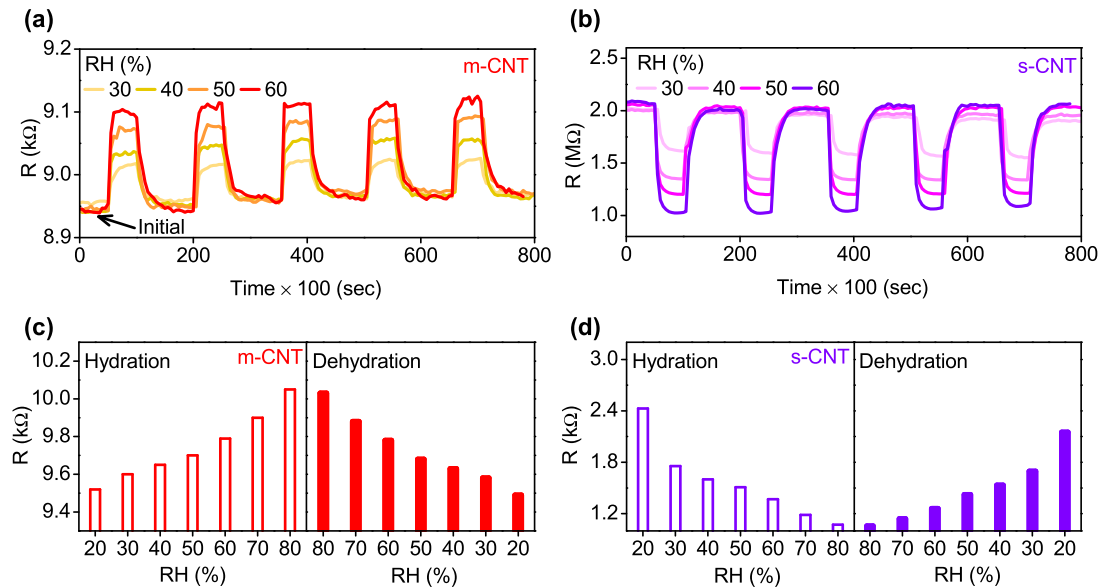
FIGURE 4. Repeatability performance of (a) m-CNT- and (b) s-CNT-based sensors at different RH levels. The hysteresis characteristic shows hydration/dehydration responses for both the (c) m-CNT- and (d) s-CNT-based sensors at varying RH levels ranging from 20 to 80%.

whereas the solid bars represent the measurement conducted during the dehydration process (sequentially decreasing the RH level from 80% to 20%). For the RH levels of 20% to 80% in 10% increments, the hysteresis of our m-CNT-based sensor was calculated as 0.31%, 0.21%, 0.20%, 0.11%, 0.19%, and 0.18%, and the maximum hysteresis value was 0.31% [43]. On the other hand, at the same RH levels, the hysteresis of the s-CNT-based sensor was 11.45%, 6.89%, 6.06%, 5.76%, 7.82%, 3.71%, and 1.31%, with a maximum hysteresis of 11.45%. It is obvious that the m-CNT-based sensor exhibits a negligible hysteresis loop during the cyclic humidity operation. However, the s-CNT-based sensor had a narrow hysteresis loop. In other words, the resistance of the s-CNT-based sensor did not completely recover during dehydration. We expect that the relatively slow recovery was due to the low concentration of H_2, which produces PdH_X, in ambient air. Analysis of these mechanisms for CNT-based sensors paves the way toward optimization of sensing performance and sensor design.

III. CONCLUSION
We demonstrated humidity sensors based on different types of CNTs, including s-CNTs and m-CNTs. To evaluate these sensors, we utilized highly purified, preseparated 99% single-walled s-CNTs and m-CNTs. We observed that the s-CNT- and m-CNT-based sensors with Pd electrodes had opposite resistance tendencies according to RH due to the difference in the dominant mechanism. It is confirmed that the dominant mechanism of the humidity response in the m-CNT-based sensor is the decrease in carrier density caused by electron charge transfer from H_2O to the CNT channel, while the dominant mechanism of humidity response in the

s-CNT-based sensor is the decrease in the Schottky barrier due to the increase in the work function of the recovered Pd electrode induced by H_2O adsorption. Therefore, we confirmed that the s-CNT-based sensor with Pd electrodes was more sensitive to H_2O adsorption than the m-CNT-based sensor with Pd electrodes due to the difference in the current dependence of changes in the Schottky barrier and carrier density. We also verified each sensing mechanism by fabricating s-CNT/m-CNT-based sensors with Cu electrodes. In addition, we confirmed that there was a difference in $\Delta R/R_0$ according to the DOS distribution of the CNTs used in the sensors, even though the sensing mechanism is the same. This study indicated that the $\Delta R/R_0$ tendency of the sensor depends on the electrode material and type of CNT. Furthermore, we confirmed that the fabricated s-CNT- and m-CNT-based humidity sensors had good repeatability. Although we demonstrated sensing experiments using only humidity, we believe that our studies can be expanded to other sensors, providing essential guidance for optimizing the design of various CNT-based sensors.

REFERENCES
[1] T. A. Blank, L. P. Eksperiandova, and K. N. Belikov, "Recent trends of ceramic humidity sensors development: A review," *Sens. Actuator B, Chem.*, vol. 228, pp. 416–422, Jun. 2016.

[2] G. Matzeu, L. Florea, and D. Diamond, "Advances in wearable chemical sensor design for monitoring biological fluids," *Sens. Actuators B, Chem.*, vol. 211, pp. 403–418, May 2015.

[3] T. Q. Trung and N.-E. Lee, "Flexible and stretchable physical sensor integrated platforms for wearable human-activity monitoringand personal healthcare," *Adv. Mater.*, vol. 28, no. 22, pp. 4338–4372, Feb. 2016.

[4] Y. Qiu and S. Yang, "ZnO nanotetrapods: Controlled vapor-phase synthesis and application for humidity sensing," *Adv. Funct. Mater.*, vol. 17, no. 8, pp. 1345–1352, Apr. 2007.

[5] Z. Wang, Y. Xiao, X. Cui, P. Cheng, B. Wang, Y. Gao, X. Li, T. Yang, T. Zhang, and G. Lu, "Humidity-sensing properties of urchinlike CuO nanostructures modified by reduced graphene oxide," *ACS Appl. Mater. Interfaces*, vol. 6, no. 6, pp. 3888–3895, Mar. 2014.

[6] D. Zhang, J. Tong, and B. Xia, "Humidity-sensing properties of chemically reduced graphene oxide/polymer nanocomposite film sensor based on layer-by-layer nano self-assembly," *Sens. Actuators B, Chem.*, vol. 197, no. 5, pp. 66–72, Jul. 2014.

[7] S. Borini, R. White, D. Wei, M. Astley, S. Haque, E. Spigone, N. Harris, J. Kivioja, and T. Ryhänen, "Ultrafast graphene oxide humidity sensors," *ACS Nano*, vol. 7, no. 12, pp. 11166–11173, Nov. 2013.

[8] T. Jalkanen, E. Mäkilä, A. Määttänen, J. Tuura, M. Kaasalainen, V.-P. Lehto, P. Ihalainen, J. Peltonen, and J. Salonen, "Porous silicon micro-and nanoparticles for printed humidity sensors," *Appl. Phys. Lett.*, vol. 101, no. 26, Dec. 2012, Art. no. 263110.

[9] W.-P. Tai and J.-H. Oh, "Fabrication and humidity sensing properties of nanostructured TiO_2–SnO_2 thin films," *Sens. Actuators B, Chem.*, vol. 85, nos. 1–2, pp. 154–157, Jun. 2002.

[10] J. Li, Y. Lu, Q. Ye, M. Cinke, J. Han, and M. Meyyappan, "Carbon nanotube sensors for gas and organic vapor detection," *Nano Lett.*, vol. 3, no. 7, pp. 929–933, Jul. 2003.

[11] T. Dürkop, S. A. Getty, E. Cobas, and M. S. Fuhrer, "Extraordinary mobility in semiconducting carbon nanotubes," *Nano Lett.*, vol. 4, no. 1, pp. 35–39, Jan. 2004.

[12] E. Artukovic, M. Kaempgen, D. S. Hecht, S. Roth, and G. Grüner, "Transparent and flexible carbon nanotube transistors," *Nano Lett.*, vol. 5, no. 4, pp. 757–760, Apr. 2005.

[13] D.-M. Sun, C. Liu, W.-C. Ren, and H.-M. Cheng, "A review of carbon nanotube-and graphene-based flexible thin-film transistors," *Small*, vol. 9, no. 8, pp. 1188–1205, Mar. 2013.

[14] J.-W. Han, B. Kim, J. Li, and M. Meyyappan, "Carbon nanotube based humidity sensor on cellulose paper," *J. Phys. Chem. C*, vol. 116, no. 41, pp. 22094–22097, Oct. 2012.

[15] M. Jeon, B. Choi, J. Yoon, D. M. Kim, D. H. Kim, I. Park, and S.-J. Choi, "Enhanced sensing of gas molecules by a 99.9% semiconducting carbon nanotube-based field-effect transistor sensor," *Appl. Phys. Lett.*, vol. 111, no. 2, Jul. 2017, Art. no. 022102.

[16] J. Wang, Z. Shi, X. Wang, X. Mai, R. Fan, H. Liu, X. Wang, and Z. Guo, "Enhancing dielectric performance of poly (vinylidene fluoride) nanocomposites via controlled distribution of carbon nanotubes and barium titanate nanoparticle," *Eng. Sci.*, vol. 4, pp. 79–86, Oct. 2018.

[17] D. Zhang, J. Sun, L. J. Lee, and J. M. Castro, "Overview of ultrasonic assisted manufacturing multifunctional carbon nanotube nanopaper based polymer nanocomposites," *Eng. Sci.*, vol. 10, pp. 35–50, May 2020.

[18] X. Yan, J. Liu, M. A. Khan, S. Sheriff, S. Vupputuri, R. Das, L. Sun, D. P. Young, and Z. Guo, "Efficient solvent-free microwave irradiation synthesis of highly conductive polypropylene nanocomposites with lowly loaded carbon nanotubes," *ES Mater. Manuf.*, vol. 9, pp. 21–33, Jul. 2020.

[19] Z. Wang, X. Li, L. Wang, Y. Li, J. Qin, P. Xie, Y. Qu, K. Sun, and R. Fan, "Flexible multi-walled carbon nanotubes/polydimethylsiloxane membranous composites toward high-permittivity performance," *Adv. Compos. Hybrid Mater.*, vol. 3, no. 1, pp. 1–7, Feb. 2020.

[20] B. J. Mapleback, T. J. Simons, Y. Shekibi, K. Ghorbani, and A. N. Rider, "Structural composite supercapacitor using carbon nanotube mat electrodes with interspersed metallic iron nanoparticles," *Electrochimica Acta*, vol. 331, Jan. 2020, Art. no. 135233.

[21] Y. Lee, B. Choi, J. Yoon, Y. Kim, J. Park, H.-J. Kim, D. H. Kim, D. M. Kim, S. Kim, and S.-J. Choi, "Highly transparent tactile sensor based on a percolated carbon nanotube network," *AIP Adv.*, vol. 8, no. 6, Jun. 2018, Art. no. 065109.

[22] P. S. Na, H. Kim, H.-M. So, K.-J. Kong, H. Chang, B. H. Ryu, Y. Choi, J.-O. Lee, B.-K. Kim, J.-J. Kim, and J. Kim, "Investigation of the humidity effect on the electrical properties of single-walled carbon nanotube transistors," *Appl. Phys. Lett.*, vol. 87, no. 9, Aug. 2005, Art. no. 093101.

[23] K.-P. Yoo, L.-T. Lim, N.-K. Min, M. J. Lee, C. J. Lee, and C.-W. Park, "Novel resistive-type humidity sensor based on multiwall carbon nanotube/polyimide composite films," *Sens. Actuators B, Chem.*, vol. 145, no. 1, pp. 120–125, Mar. 2010.

[24] L. Liu, X. Ye, K. Wu, R. Han, Z. Zhou, and T. Cui, "Humidity sensitivity of multi-walled carbon nanotube networks deposited by dielectrophoresis," *Sensors*, vol. 9, no. 3, pp. 1714–1721, Mar. 2009.

[25] C. L. Cao, C. G. Hu, L. Fang, S. X. Wang, Y. S. Tian, and C. Y. Pan, "Humidity sensor based on multi-walled carbon nanotube thin films," *J. Nanomater.*, vol. 2011, Jan. 2011, Art. no. 707303.

[26] S. Ishihara, C. J. O'Kelly, T. Tanaka, H. Kataura, J. Labuta, Y. Shingaya, T. Nakayama, T. Ohsawa, T. Nakanishi, and T. M. Swager, "Metallic versus semiconducting SWCNT chemiresistors: A case for separated SWCNTs wrapped by a metallosupramolecular polymer," *ACS Appl. Mater. Interfaces*, vol. 9, no. 43, pp. 38062–38067, Oct. 2017.

[27] Z. Zhao, M. Knight, S. Kumar, E. T. Eisenbraun, and M. A. Carpenter, "Humidity effects on Pd/Au-based all-optical hydrogen sensors," *Sens. Actuators B, Chem.*, vol. 129, no. 2, pp. 726–733, Feb. 2008.

[28] C. Wang, J.-C. Chien, K. Takei, T. Takahashi, J. Nah, A. M. Niknejad, and A. Javey, "Extremely bendable, high-performance integrated circuits using semiconducting carbon nanotube networks for digital, analog, and radio-frequency applications," *Nano Lett.*, vol. 12, no. 3, pp. 1527–1533, Feb. 2012.

[29] J. Liu, M. J. Casavant, M. Cox, D. A. Walters, P. Boul, W. Lu, A. J. Rimberg, K. A. Smith, D. T. Colbert, and R. E. Smalley, "Controlled deposition of individual single-walled carbon nanotubes on chemically functionalized templates," *Chem. Phys. Lett.*, vol. 303, nos. 1–2, pp. 125–129, Apr. 1999.

[30] B. Kitiyanan, W. E. Alvarez, J. H. Harwell, and D. E. Resasco, "Controlled production of single-wall carbon nanotubes by catalytic decomposition of CO on bimetallic Co–Mo catalysts," *Chem. Phys. Lett.*, vol. 317, nos. 3–5, pp. 497–503, Feb. 2000.

[31] M. C. Hersam, "Progress towards monodisperse single-walled carbon nanotubes," *Nature Nanotechnol.*, vol. 3, no. 7, pp. 387–394, Jul. 2008.

[32] L. Greenspan, "Humidity fixed points of binary saturated aqueous solutions," *J. Res. Nat. Bur. Stand.*, vol. 81A, no. 1, pp. 89–96, Feb. 1977.

[33] S. Dixit, A. Srivastava, R. K. Shukla, and A. Srivastava, "ZnO thick film based opto-electronic humidity sensor for a wide range of humidity," *Opt. Rev.*, vol. 14, no. 4, pp. 186–188, Jul. 2007.

[34] P. G. Collins, "Extreme oxygen sensitivity of electronic properties of carbon nanotubes," *Science*, vol. 287, no. 5459, pp. 1801–1804, Mar. 2000.

[35] D. Kang, N. Park, J.-H. Ko, E. Bae, and W. Park, "Oxygen-induced p-type doping of a long individual single-walled carbon nanotube," *Nanotechnology*, vol. 16, no. 8, pp. 1048–1052, May 2005.

[36] J. Melcher, Y. Daben, and G. Ark, "Dielectric effects of moisture in polyimide," *Trans. Elect. Insul.*, vol. 24, no. 1, pp. 31–38, Feb. 1989.

[37] S. Dekura, H. Kobayashi, K. Kusada, and H. Kitagawa, "Hydrogen in palladium and storage properties of related nanomaterials: Size, shape, alloying, and metal-organic framework coating effects," *ChemPhysChem*, vol. 20, no. 10, pp. 1158–1176, Apr. 2019.

[38] C. Das, Z. Mohammad, and M. M. Alam, "Optical hydrogen gas sensor based on palladium coated microring resonator," in *Proc. Int. Conf. Innov. Eng. Technol. (ICIET)*, Dec. 2018, pp. 1–5.

[39] Y. Sun and H. H. Wang, "High-performance, flexible hydrogen sensors that use carbon nanotubes decorated with palladium nanoparticles," *Adv. Mater.*, vol. 19, no. 19, pp. 2018–2823, Aug. 2007.

[40] D. R. Kauffman, C. M. Shade, H. Uh, S. Petoud, and A. Star, "Decorated carbon nanotubes with unique oxygen sensitivity," *Nature Chem.*, vol. 1, no. 6, pp. 500–506, Aug. 2009.

[41] S. Kazaoui, N. Minami, R. Jacquemin, H. Kataura, and Y. Achiba, "Amphoteric doping of single-wall carbon-nanotube thin films as probed by optical absorption spectroscopy," *Phys. Rev. B, Condens. Matter*, vol. 60, no. 19, pp. 13339–13342, Nov. 1999.

[42] C. Y. Lee, S. Baik, J. Zhang, R. I. Masel, and M. S. Strano, "Charge transfer from metallic single-walled carbon nanotube sensor arrays," *J. Phys. Chem. B*, vol. 110, no. 23, pp. 11055–11061, Jun. 2006.

[43] X. Zhang, D. Maddipatla, A. K. Bose, S. Hajian, B. B. Narakathu, J. D. Williams, M. F. Mitchell, and M. Z. Atashbar, "Printed carbon nanotubes-based flexible resistive humidity sensor," *IEEE Sensors J.*, vol. 20, no. 21, pp. 12592–12601, Nov. 2020.

YONGWOO LEE received the B.S. degree in electrical engineering from the School of Electrical Engineering, Kookmin University, Seoul, South Korea, where he is currently pursuing the Ph.D. degree.

JINSU YOON received the M.S. and Ph.D. degrees in electrical engineering from the School of Electrical Engineering, Kookmin University, Seoul, South Korea.

YEAMIN KIM received the B.S. and M.S. degrees in electrical engineering from the School of Electrical Engineering, Kookmin University, Seoul, South Korea.

DONG MYONG KIM (Member, IEEE) received the B.S. *(magna cum laude)* and M.S. degrees in electronics engineering from Seoul National University, Seoul, South Korea, in 1986 and 1988, respectively, and the Ph.D. degree in electrical engineering from the University of Minnesota, Twin Cities, MN, USA, in 1993. Since 1993, he has been a Professor with the School of Electrical Engineering, Kookmin University, Seoul. His research interest includes the modeling and characterization of semiconductor devices.

DAE HWAN KIM (Senior Member, IEEE) received the B.S., M.S., and Ph.D. degrees in electrical engineering from Seoul National University, Seoul, South Korea, in 1996, 1998, and 2002, respectively. He is currently a Professor with the School of Electrical Engineering, Kookmin University, Seoul, South Korea. His current research interests include nanoCMOS, oxide and organic thin-film transistors, biosensors, and neuromorphic devices.

SUNG-JIN CHOI received the M.S. and Ph.D. degrees in electrical engineering from the Korea Advanced Institute of Science and Technology, Daejeon, South Korea, in 2012. He is currently an Associate Professor with the School of Electrical Engineering, Kookmin University, Seoul, South Korea.

• • •